3-Dimensional Simulation of the Grain Formation in Investment Castings

Ch.-A. GANDIN, M. RAPPAZ, and R. TINTILLIER

A 3-dimensional (3-D) probabilistic model which has been developed previously for the prediction of grain structure formation during solidification is applied to thin superalloy plates produced using the investment-casting process. This model considers the random nucleation and orientation of nuclei formed at the mold surface and in the bulk of the liquid, the growth kinetics of the dendrite tips, and the preferential growth directions of the dendrite trunks and arms. In the present study, the grains are assumed to nucleate at the surface of the mold only. The computed grain structures, as observed in 2-dimensional (2-D) sections made parallel to the mold surface, are compared with experimental micrographs. The grain densities are then deduced as a function of the distance from the mold surface for both the experiment and the simulation. It is shown that these values are in good agreement, thus, providing validation of the grain formation mechanisms built into the 3-D probabilistic model. Finally, this model is further extended to more complex geometries and the 3-D computed grain structure of an equiaxed turbine-blade airfoil is compared with the experimental transverse section micrograph.

I. INTRODUCTION

PROBABILISTIC modeling of grain structure formation in castings has received increased attention since the original work of Brown and Spittle.[1,2] These authors adapted a Monte Carlo method previously developed by Anderson *et al.*[3,4] for the simulation of grain growth in solids to the particular case of solidification. Based upon a minimization principle of the interfacial energy of the grains (Potts model), this method considers a 2-dimensional (2-D) hexagonal network of sites, each having a grain index number. The grains can grow by allowing transitions between unlike sites to occur during a Monte Carlo time step. Although Brown and Spittle were able to produce grain structures which were close to those observed in real castings, their method is not based upon the physical mechanisms of dendrite growth formation as explained in literature elsewhere.[5] In particular, it does not specifically consider the mechanisms responsible for grain formation in dendritic alloys, *i.e.*, the growth kinetics of the dendrite tips, the preferential ⟨100⟩ growth direction of dendrite trunks and arms, and the branching mechanisms at grain boundaries or near the mold surface.[6,7,8] Furthermore, their approach was only 2-D. The variations of this method proposed recently by Zhu and Smith[9,10] do not remove these limitations.

Rappaz and Gandin[5] have proposed a different probabilistic approach for the simulation of grain structure formation in solidification processes. Their method, based upon a cellular automaton (CA) technique,[11] considers the random aspects associated with the location and crystallographic orientation of new nuclei formed either in the bulk of the liquid or at the mold wall surface. The growth of the ⟨100⟩ dendrites is specifically taken into account when simulating the "capture" of neighboring liquid cells by a growing grain. Although the method was limited to small specimens of uniform temperature, the predicted grain structures were close to experimental micrographs. Furthermore, the influence of the inoculation parameters, cooling rate, and alloy concentration on the columnar-to-equiaxed transition (CET) could be simulated in a quantitative way.

In another article, Gandin *et al.*[12] showed that their 2-D CA model could not reproduce all of the details seen in experimental section micrographs of thin-plate superalloy investment castings. Although the CET was correctly predicted in the various plates, the appearance of the corresponding columnar zones (*i.e.*, of the zones formed by the grains nucleated at the surface of the mold) was quite different. Extending their model to three dimensions, Gandin *et al.*[12] were able to show that these differences could be explained by stereological effects associated with those grains which nucleate at the surface of the mold but not in the plane of the section micrograph. The 2-D transverse sections of the computed three-dimensional grain structures were compared with the grain structures computed with the 2-D model and with experimental section micrographs. From this comparison, it appeared that the 3-D aspects of the dendritic growth are important when modeling the grain structures in castings.

In the present contribution, the 3-D probabilistic model of Gandin *et al.*[12] is further validated by comparing quantitatively the experimental and computed grain structures in thin-plate superalloy castings, as observed in 2-D sections made parallel to the mold surface. From these observations, the computed and experimental surface densities of the grains are calculated as a function of the distance from the mold surface. It is shown that these values are in good agreement, thus providing another validation of the grain formation mechanisms built in the 3-D probabilistic model. Finally, this

Ch.-A. GANDIN, Graduate Student, and M. RAPPAZ, Professor, are with the Département des Matériaux, Ecole Polytechnique Fédérale de Lausanne, MX-G Ecublens, 1015 Lausanne, Switzerland. R. TINTILLIER, Foundry Research Engineer, is with the Département Matériaux et Procédés-Direction Technique, Société Nationale d'Etude et de Construction de Moteurs d'Aviation, 92230 Gennevilliers, France.

Manuscript submitted April 12, 1993.

model is further extended to more complex geometries, and the 3-D computed grain structure of a nondirectionally solidified (NDS) turbine-blade airfoil is compared with the experimental transverse section micrograph. In the literature, the word "equiaxed" turbine blade is usually used to label investment castings which are not produced by directional solidification (DS) or single-crystal (SC) technologies. As shown in Reference 12, the word equiaxed might be abusive since the grains, which might indeed be very fine and appear as equiaxed at the part surface, still originate from the mold wall surface. These grains grow toward the inside of the casting and thus result in a columnar zone whose extent is determined by the local thermal solidification parameters or by the thickness of the part itself. For that reason, NDS rather than "equiaxed" will be chosen here in order not to confuse the reader.

II. EXPERIMENT

The thin parallelepiped-shape plate and the turbine blade were produced using the investment-casting process. The internal surface of the ceramic mold was coated with inoculant particles in order to enhance heterogeneous nucleation at the surface. The industrial alloy was the nickel-base INCO718* with principle alloying elements of 21 pct Cr, 20.5 pct Fe, 5.5 pct Nb, 3.3 pct Mo, 1.15 pct Ti, and 0.7 pct Al (wt pct). After solidification, the plate and the airfoil were cut along a transverse section (*i.e.*, perpendicular to its largest surface). Serial grinding of the plate was also made parallel to the largest surface of the casting in order to observe the evolution of the grain structure as a function of the distance from the mold wall. The observation planes were mechanically polished and electrolytically etched with Kalling reagent solution in order to reveal the grain contours. The grain density in the parallel sections of the plate was measured using the ASTM procedure no. E112-77 (the number of grains measured for each section was greater than 50).

*INCO718 is a trademark of Inco Alloys International, Inc., Huntington, WV.

In a former analysis,[12] it was shown that, under these casting conditions, the grain structure was wholly columnar (*i.e.*, all of the grains had been nucleated at the mold wall) in 1- and 3-mm-thick plates, whereas a few truly equiaxed grains could be observed at the center of a 10-mm-thick plate. In order to observe the selection mechanism which operates along the columnar zone, a 1.5-mm-thick plate was chosen in the present serial sectioning investigation. The maximum thickness of the blade airfoil was 3 mm. For such a thickness, it was assumed that the temperature distribution across the plate and the blade was uniform (*i.e.*, small Biot number).

III. 3-D PROBABILISTIC MODEL

The probabilistic model which was used to simulate the dendritic grain structure of the INCO718 plate and airfoil castings has already been explained in Reference 12. For this reason, it will only be briefly summarized here.

The 3-D domain to be modeled was first decomposed into a regular network of cells (Figure 1). In the present case, a regular arrangement of cubic cells was chosen, and the six nearest neighbors of each cell were identified. Since not all of the plate or airfoil were simulated, periodic boundary conditions were applied at the boundaries inside the metal itself (*e.g.*, cells located at the upper frontier of the airfoil portion in Figure 1 had their upper neighbor located at the bottom boundary). All the cells which were contiguous with the mold wall were identified with a reference index; these cells were characterized by a heterogeneous nucleation law typical of the mold wall (shown later). It was shown in a previous study[12] that, for thin-plate investment castings, the grain structure can be explained in terms of heterogeneous nucleation at the mold wall only (*i.e.*, "columnar" grains), and thus, no nucleation law for the heterogeneous nucleation in the bulk of the liquid was defined in the present study.

Nucleation at the surface of the mold (*i.e.*, for the cells located near the mold wall) was set to occur at a critical "burst" undercooling, ΔT_N. Because the growth rate of the dendrite tips is a quadratic function of the undercooling, the small value given to the parameter, ΔT_N, is unimportant since it only delays the time at which the dendritic grains start to grow significantly. If ΔT_N becomes too large, however, the thermal history of the casting could be affected (recalescence) and/or equiaxed grains could nucleate in the bulk of the liquid. Therefore, this undercooling was chosen with an arbitrary small value (0.5 °C) in order to account for the inoculant coating deposited on the interior wall of the ceramic mold. The surface density of these nuclei, n_s (m^{-2}), which is the important parameter of the model, was estimated from the experiment as described in more details in the Results section.

At the beginning of the simulation, all the cells were

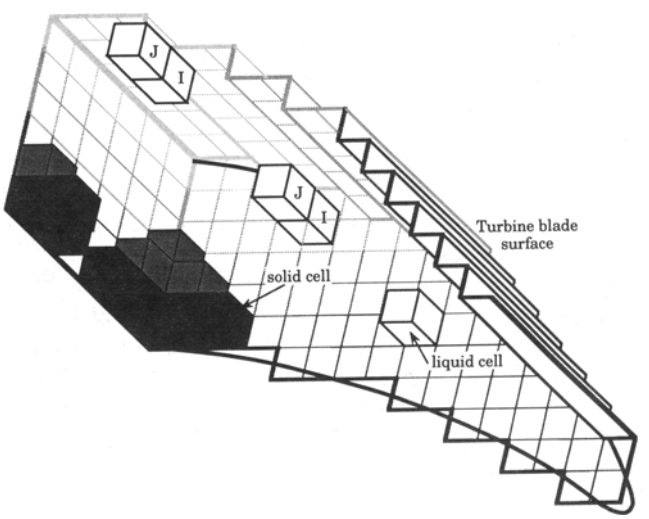

Fig. 1—Schematics of the 3-D probabilistic model used to simulate the dendritic grain structure formation in a small portion of a turbine-blade airfoil.

liquid. In a time-stepping calculation, the uniform temperature of the casting was decreased according to a simple heat balance of the specimen. A heat transfer coefficient between the metal and the ceramic mold was taken into account, and the initial temperatures of the metal and mold were set to the pouring and preheat temperatures, respectively. The value of this coefficient was estimated from previous experiments.[12] When the critical undercooling ΔT_N was reached, a number of cells, $N_c = n_s \cdot S$, were chosen randomly among all the cells located near the mold wall surface. The term S is the total surface of the casting in contact with the ceramic mold and simulated using the probabilistic model (Figure 1). When a cell solidified by nucleation, its index number, which was zero when it was liquid, was set to a positive integer randomly chosen among 976 classes. Each class corresponded to a particular set of the three Euler angles, $\{\theta, \phi, \psi\}$, characterizing the $\langle 100 \rangle$ crystallographic orientations of the grains in the reference frame attached to the cells' network.[12] It should be noted that, for a curved surface such as the shape of the airfoil shown in Figure 1, the cell density at the surface is not uniform. When the surface is locally parallel to two main directions of the cells' network, the surface density of the cells is simply given by d^{-2}, where d is the spacing of the cubic network. When the surface is turned 45 deg with respect to one of the network directions (*i.e.*, [110] plane of the cells' network), the local density of cells is equal to $d^{-2}/\sqrt{2}$, as a result of approximating an inclined smooth surface with a corrugated arrangement of cells. This effect, which could only slightly modify the simulation result for the airfoil, was not taken into account in choosing the "nucleation" cells.

Once a new nucleus had formed at a particular cell location, it was assumed to grow as an octahedron with main diagonals corresponding to the $\langle 100 \rangle$ crystallographic orientations. It should be kept in mind that this assumption is a consequence of three more basic hypotheses:[12] (1) the incubation time necessary for a spherical nucleus to become dendritic is negligible; (2) the growth kinetics of the dendrite arms is given by that of an isolated tip (*i.e.*, the incubation time necessary for a dendrite arm to "escape" from its neighbors is negligible); and (3) the temperature is uniform. Since the growth of these diagonals is driven by the dendrite tips, their half-length at time t, $L(t)$, is given by the following:

$$L(t) = \int_{t_N}^{t} v[\Delta T(t')] \cdot dt' \qquad [1]$$

where t_N is the time of nucleation of the grain, and $v(\Delta T)$ is the growth kinetics of the dendrite tip, which is a function of the undercooling, ΔT. As explained in Reference 12, the growth kinetics of the dendrite tip, *i.e.*, the relationship $v(\Delta T)$, for the INCO718 alloy can be deduced from the marginal stability criterion extended to multicomponent alloys. In order to speed up the probabilistic model calculations, a simple polynomial function was then fitted to the following theoretical predictions:

$$v(\Delta T) = a_2 \cdot \Delta T^2 + a_3 \cdot \Delta T^3 \qquad [2]$$

Table I. Heterogeneous Nucleation and Growth Kinetics Parameters Used for the Simulation of the INCO718 Investment Castings

Surface grain density, n_s (Figs. 2 through 4)	5.8×10^8 m^{-2}
Surface grain density, n_s (Fig. 5)	7.3×10^6 m^{-2}
Growth parameter, a_2 (Eq. 2)	1.691×10^{-7} m·s^{-1}·K^{-2}
Growth parameter, a_3 (Eq. 2)	4.148×10^{-7} m·s^{-1}·K^{-3}

The value of these coefficients is given in Table I, together with the grain density, n_s, deduced for the surfaces of the 1.5-mm-thick plate and of the turbine blade. It should be noted that the difference seen for the two values of n_s arises from the different solidification conditions (melt superheat, preheating of the mold, and gating system) used to cast the two specimens.

The growth algorithm is then equivalent to finding, at each time step, which are the liquid cells that have been captured by the growing grains of octahedral shape. The index number of all the cells being captured by a given grain is set to the index number of the corresponding nucleus.

IV. RESULTS

Figure 2(a) reproduces the grain structure seen in a transverse section of the 1.5-mm-thick INCO718 plate. As already discussed,[12] some grains are directly connected to the surface of the casting in the plane of the micrograph. For such grains, it is clear that they have been heterogeneously nucleated at the mold wall. In Figure 2(a), there are also grains which are not directly linked to the edge of the casting. Although such grains could be thought of as having nucleated in the bulk of the liquid, their elongated appearance rather suggests that they also have nucleated at the surface of the ceramic mold, but not necessarily in the plane of the section micrograph. Although serial sectioning with a clear identification of each grain is the only experimental means to unambiguously validate such a conjecture, the 3-D probabilistic model briefly described in Section I is a simple and powerful tool to analyze stereological effects associated with such grain structures. Figure 2(b) shows a similar transverse 2-D section of the computed 3-D grain structure using the probabilistic model and the nucleation growth parameters listed in Table I. As can be seen, the simulation also predicts grains which are not directly connected to the surface of the casting in the observation plane, even though only the heterogeneous nucleation at the mold surface was considered in the calculations.

When the experimental and simulated micrographic sections of Figure 2 are examined in detail, it appears that the lateral extension of the grains (*i.e.*, dimension parallel to the mold wall) increases with increasing distance from the mold wall. While it is well known[6,7] that the grain size increase is due to the competition between grains of different crystallographic orientations, the grains which have one of their $\langle 100 \rangle$ directions most closely aligned normal with the surface mold grow preferentially at the expense of grains having a less favorable

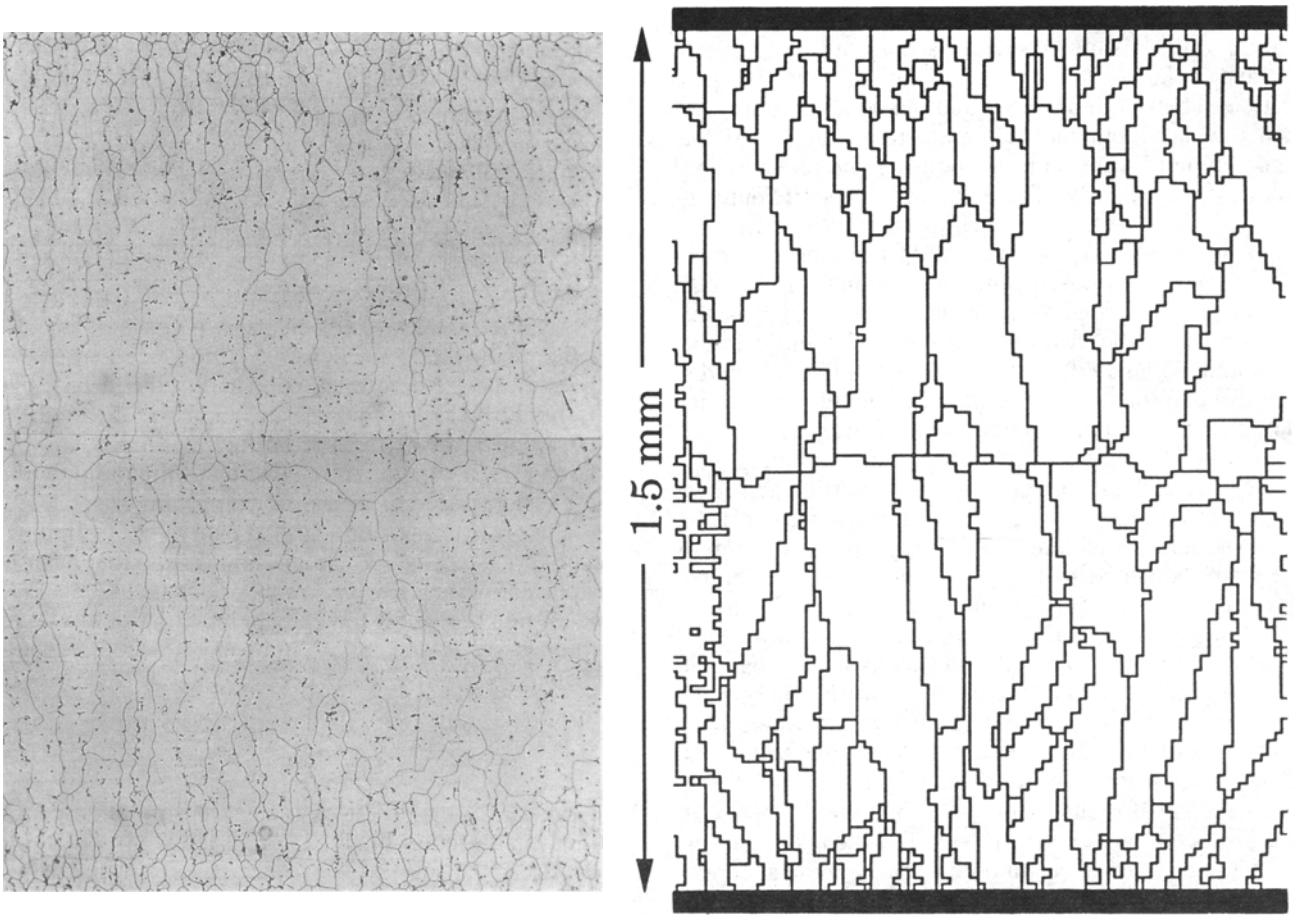

(*a*) (*b*)

Fig. 2—(*a*) Experimental and (*b*) simulated grain structure in a transverse section of a 1.5-mm-thick INCO718 plate.

orientation. The physical mechanism of this grain selection has been observed by Esaka *et al.* on organic alloys.[8] It appears that the grain boundary of two grains having converging ⟨100⟩ orientations is locked, whereas, for diverging ⟨100⟩ directions, branching mechanisms of dendrite arms in the open region of liquid, which continuously formed at the grain boundary, are responsible for this selection (see for example Figure 2 of Reference 5 for a graphic explanation). In the present 3-D probabilistic model, the grain competition in a uniform temperature situation is simulated through the use of an octahedral shape of the grains. If the grains were spherical in shape (isotropic growth), a burst nucleation at ΔT_N could only produce planar grain boundaries[13] perpendicular to the mold surface and, accordingly, no grain selection in plate geometries.*

*In the case of isotropic growth and burst nucleation, a grain selection would occur according to the geometry of the casting: in concave regions, grains would increase in size, whereas they would shrink, and possibly disappear, in convex parts.

In order to further verify the predictions of the probabilistic model and more specifically the criterion of grain selection induced by the octahedral shape, a quantitative measurement of the grain density in sections parallel to the mold surface was made. These densities ($n_s(z)$), measured at two different locations of the same plate, are reported in Figure 3 as a function of the distance (z) from the mold wall. Since these grains are columnar, no stereological correction was introduced, and the values reported on the vertical axis of this figure are directly the as-measured surface densities. It can be seen that the experimental values present some scattering. This sensitivity to the plate location is attributed to the mold-filling stage. Variations in the heat and mass transport and possibly crystallite redissolution could explain the differences seen in the grain density with respect to the location in the plate. The mold filling not only affects the local inoculation conditions but can also modify the local temperature history. In particular, it can induce a thermal gradient across the plate even though the Biot number is small. None of these effects is taken into account in the probabilistic model.

The dotted curve shown in Figure 3 corresponds to the evolution of the grain density as calculated with the probabilistic model. Besides the measured cooling curve and the growth kinetics of the dendrite tips which has been calculated for the multicomponent alloy, the only adjustable parameter of the model is the grain density at the surface of the plate (the undercooling at which nucleation occurs has almost no effect as explained before). This latter value was deduced using a linear

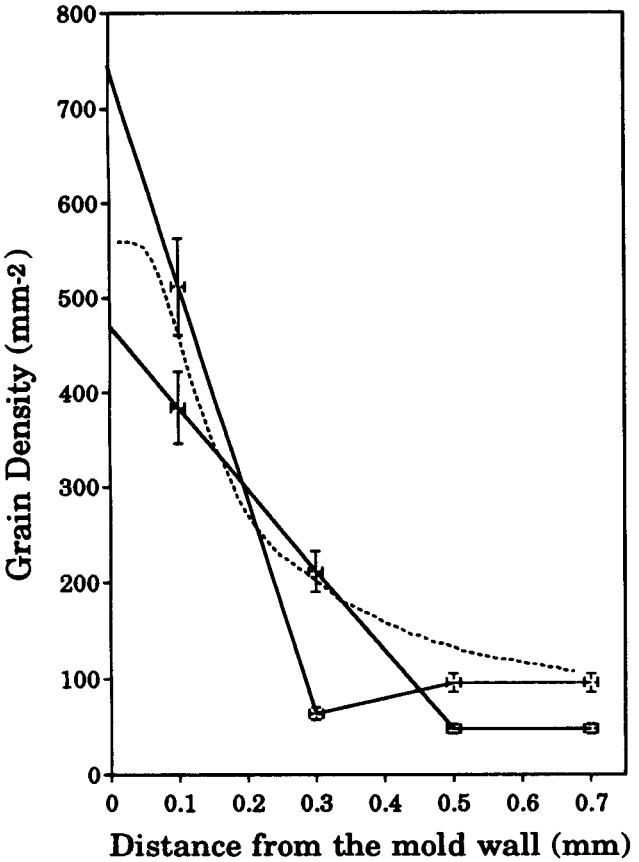

Fig. 3—Experimental grain density measured in two different places of the 1.5-mm-thick INCO718 plate casting as a function of the distance from the mold wall (plain curves). These values can be compared with the grain density predicted with the probabilistic model (dotted curve).

interpolation based upon the grain densities measured at 0.1 and 0.3 mm from the mold wall, and the average was taken from these two measurement locations. The values $n_s = n_s(z = 0)$ (Table I) were then used in the simulation. As can be seen in Figure 3, the predicted evolution of the grain density as a function of the distance from the mold agrees fairly well with the measurement. In particular, both the experiment and the simulation indicate that the grain density varies by at least a factor of 3 to 4 over a very short distance (typically 0.7 mm) as a result of the grain selection mechanisms. The grain selection predicted by the model seems to be less pronounced than that deduced from the experimental curves. However, it should be kept in mind that no quantitative measurement of the grain density was made at depths smaller than 100 μm and that the straight lines drawn for the experimental curves near the surface of the mold ($z = 0$) are extrapolated from the first two points ($z = 100$ μm and $z = 300$ μm). The flat plateau of the predicted curve, $n_s(z)$, near $z = 0$ seems to be associated with the finite resolution of the cellular automaton rather than with a physical mechanism. It should be noted that the simulation result shown in Figure 3 comes from a unique calculation but is already an average over several hundreds of grains, *i.e.*, over a large number of grain boundary configurations.

Figures 4(a) and (b) show the computed grain structures in sections parallel to the mold surface at 0.1 and 0.7 mm, respectively, from the mold wall. The variations of the grain density as a function of the distance from the surface of heterogeneous nucleation clearly appear in these figures.

Finally, in order to show that the 3-D model can also be applied to more complex shape castings, the 3-D grain structure has been computed for a portion of an NDS turbine-blade airfoil (see also Figure 1 of Reference 12). A 2-D transverse section of this computed grain structure is compared with the experimental section micrograph in Figure 5. Figure 5(a) shows the experimental section micrograph, whereas the grain contour has been redrawn in Figure 5(b) from a clear identification of the grains. The computed grain morphology and size shown in Figure 5(c) generally compares well with the experimental structures reproduced in Figure 5(b). The parting line corresponding to the meeting of the columnar growth fronts has a similar aspect and position in both the computed and experimental structures. Only detailed observation of the leading and trailing edges of the blade airfoil reveal a difference in the grain density and, thus, in the grain structure appearance.

V. CONCLUSION

The grain structure of a thin-plate superalloy investment casting was simulated with a probabilistic model, and quantitative metallography was performed on both the experimental and simulated section micrographs. The overall appearance of the predicted grain structure and the columnar-to-equiaxed transition were shown to be well reproduced by the model in a previous article.[12] In the present contribution, it was further demonstrated that the evolution of the grain density at an increasing distance from the place of nucleation (*i.e.*, the mold surface) can be predicted by the model quite accurately. Such quantitative measurements further support the grain formation mechanisms which have been integrated in the probabilistic model. In uniform temperature situations, this selection of grains in the columnar zone is simply introduced *via* the octahedral shape of the dendritic grains. Such shapes, equivalent to squares in 2-D, have already been observed by Ovsienko *et al.*[15] in the case of cyclohexanol crystal growth. The following physical background which underlies such an octahedral shape was previously discussed:[5,12] uniform temperature situation, ⟨100⟩ growth directions of the dendrite tips and arms, and negligible incubation time for a spherical nucleus to become unstable and for a dendrite arm to grow freely into the liquid no longer feeling the solute boundary layers of the neighboring arms. It has also been shown in this article that the model can be adapted easily to more complex shape castings such as a portion of a turbine-blade airfoil. For 2-D geometries, the growth algorithm has already been modified to encompass nonuniform temperature situations and predict the extension of a single-dendritic grain near a re-entrant corner of a turbine blade.[14] Beside metallography analysis, further validation of the model regarding the evolution of the crystallographic texture of the grains is under progress. The limitations of the model which have been pointed

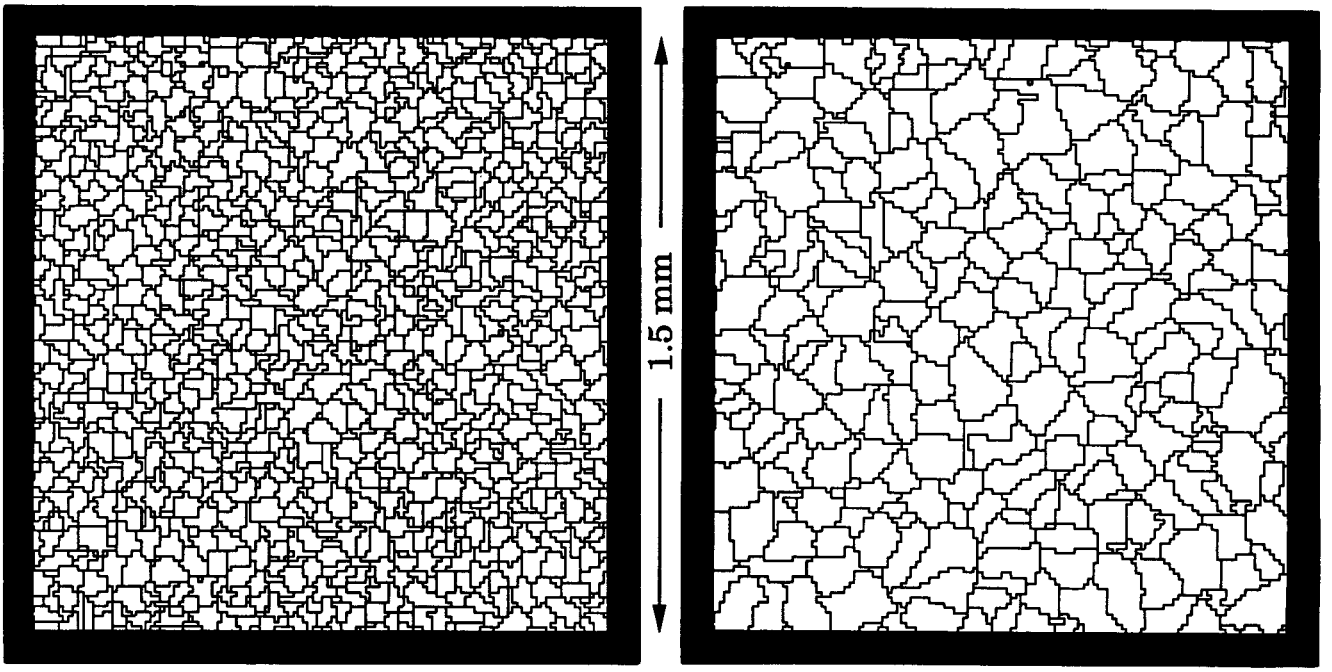

Fig. 4—Simulated grain structure of a 1.5-mm-thick INCO718 plate in two sections parallel to the mold surface at (*a*) 0.1 mm and (*b*) 0.7 mm from the mold.

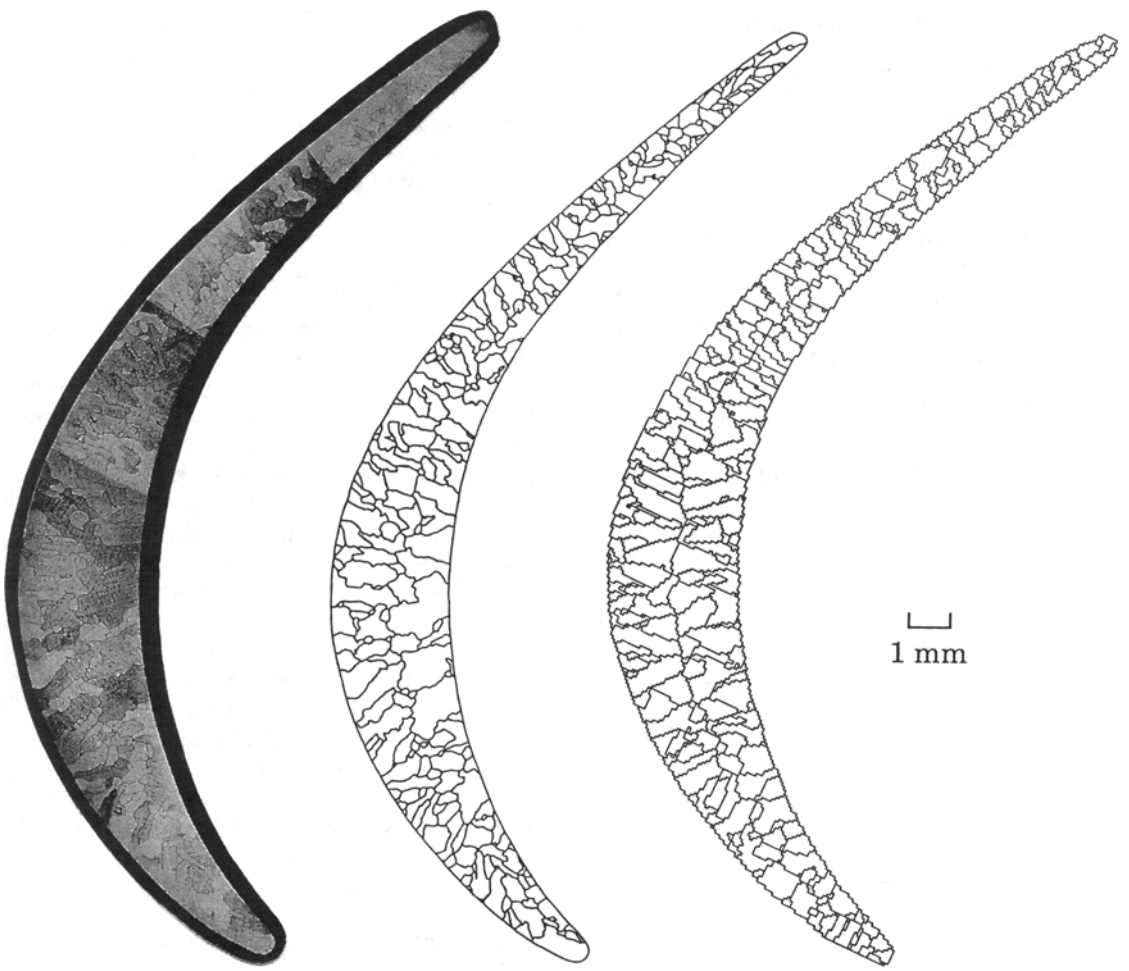

Fig. 5—Experimental micrographic (*a*) cross section (*b*) grain contours and (*c*) simulated grain structures in a transverse section of an INCO718 turbine-blade airfoil.

out are those associated with convection and mold filling. Fluid flow can indeed modify the local inoculation and growth conditions. It can also transport equiaxed grains formed in the bulk of the liquid and/or enhance this latter growth morphology by dendrite arm detachment.

ACKNOWLEDGMENTS

The authors would like to thank SNECMA for providing a financial contribution to this research and for the use of their experimental foundry equipment. The financial support of the Commission pour l'Encouragement de la Recherche Scientifique, Bern, is also greatly acknowledged.

REFERENCES

1. S.G.R. Brown and J.A. Spittle: *Mater. Sci. Technol.*, 1989, vol. 5, pp. 362-68.
2. J.A. Spittle and S.G.R. Brown: *Acta Metall.*, 1989, vol. 37, pp. 1803-10.
3. M.P. Anderson, D.J. Srolovitz, G.S. Grest, and P.S. Sahni: *Acta Metall.*, 1984, vol. 32, pp. 783-91; D.J. Srolovitz, M.P. Anderson, P.S. Sahni, and G.S. Grest, vol. 32, pp. 793-802; D.J. Srolovitz, M.P. Anderson, G.S. Grest, and P.S. Sahni, vol. 32, pp. 1429-38; G.S. Grest, D.J. Srolovitz, and M.P. Anderson, 1985, vol. 33, pp. 509-20; D.J. Srolovitz, G.S. Grest, and M.P. Anderson, 1985, vol. 33, pp. 2233-47.
4. M.P. Anderson, G.S. Grest, and D.J. Srolovitz: *Phil. Mag. B*, 1989, vol. 59, pp. 293-329.
5. M. Rappaz and Ch.A. Gandin: *Acta Metall.*, 1993, vol. 41, pp. 345-60.
6. B. Chalmers: *Principles of Solidification*, John Wiley & Sons, New York, NY, 1964.
7. W. Kurz and D.J. Fisher: *Fundamentals of Solidification*, Trans Tech Publications, Aedermannsdorf, Switzerland, 1989.
8. H. Esaka, W. Kurz, and R. Trivedi: *Solidification Processing*, Institute of Metals, London, 1988, pp. 198-201.
9. P. Zhu and W. Smith: *Acta Metall.*, 1992, vol. 40, pp. 683-92.
10. P. Zhu and W. Smith: *Acta Metall.*, 1992, vol. 40, pp. 3369-79.
11. H.W. Hesselbarth and I.R. Göbel: *Acta. Metall.*, 1991, vol. 39, pp. 2135-43.
12. Ch.-A. Gandin, M. Rappaz, and R. Tintillier: *Metall. Trans. A*, 1993, vol. 24A, pp. 467-79.
13. Ch. Charbon and M. Rappaz: *Mater. Sci. Eng.*, 1993, vol. 1, pp. 455-66.
14. Th. Imwinkelried, J.-L. Desbiolles, Ch.-A. Gandin, M. Rappaz, S. Rossmann, and Ph. Thévoz: in *Modeling of Casting, Welding and Advanced Solidification Processes*, T.S. Piwonka, V. Voller, and L. Katgerman, eds., TMS, Warrendale, PA, 1993, pp. 63-70.
15. D.E. Ovsienko, G.A. Alfintsel, and V.V. Maslov: *J. Cryst. Growth*, 1974, vol. 26, p. 233.